Desalination and Water Treatment
www.deswater.com

doi: 10.5004/dwt.2020.25282

187 (2020) 47–55
May

Safety assessment of piping induced by crossing pipeline engineering

Jie Yang[a,b], Ming Yue[c], Xinwei Song[b], Dongmei Shen[b], Luxiu Chai[b], Wanfen Wang[b,*]

[a]*College of Civil Engineering, Hefei University of Technology, Hefei, Anhui 230009, China*
[b]*Department of Architecture and Civil Engineering, West Anhui University, Lu'an, Anhui 237012, China, email: 181592579@qq.com (W. Wang)*
[c]*Civil and Environmental Engineering School, University of Science and Technology Beijing, Beijing 100083, China*

Received 7 July 2019; Accepted 15 December 2019

ABSTRACT

The landslide deformation of the dam foundation is caused mainly by the seepage of the piping effect. In order to evaluate whether the pipeline crossing project would induce piping or not, according to the regional engineering geological conditions and the factors such as flood and river erosion, the hydrogeological conditions, generalization and mathematical modeling of crossing pipeline through Hangbu River project in central Anhui province are carried out, and then proceed numerical simulation of groundwater flow field in certain region based on Modflow software. The results showed that the channel was scoured obviously under the conditions of designed flood, however, the maximum hydraulic gradient of the groundwater flow field in the crossing section of pipeline engineering was less than the critical hydraulic gradient which could disturb sand grains, therefore, the river bed scour in flood season would not cause the seepage damage of the project.

Keywords: Piping; Hydraulic conductivity; Critical hydraulic gradient; Pipeline crossing; Numerical model

1. Introduction

Piping is one of the main forms of groundwater seepage failure which usually occurs at earth embankments in flood season. It is often presented the process of migration and loss of soil particles under seepage in engineering, then the loss of particles from the surface of the soil is gradually extended upstream to form an irregular pipe path [1–3]. The research on the phenomenon of piping is the focal point of hydraulic structure and underground seepage, many scholars have done a lot of work. Chen et al. [4] simulated the piping destruction processes of multilayer embankment with different kinds of sand layers based on the laboratory tests and analyzed the effect of sand layers with different grain-size distributions on the mechanism and process of the occurrence of piping. Liu et al. [5] studied the seepage failure mechanism of double-layer stratum structure according to the permeability coefficient ratio. Liang et al. [6], Li and Zhou [7], and Zhou et al. [8] studied the development of piping through simulation experiments of sand tank and visual tracking technology, respectively. Wang et al. [9] built equation of fluid pressure according to the flow conservation, and then used the modified algorithm to simulate the unsteady seepage process; Ubilla et al. [10] investigated the failure of the levees and floodwall as a result of piping in Louisana and surrounding areas during Hurricane Katrina. Fujisawa et al. [11] simulated the temporal alteration and the spatial distribution of porosity and predicted the typical development of piping within an embankment. Zhou et al. [12] produced a laboratory model that could depict how fine particles were eroded from the soil fabric and transported out of the soil mass. Wang et al. [13] used a numerical model to simulate the pipe progression in a levee foundation, analyzed the inception, and transportation of erodible particles from the soil fabric. Ojha and Singh [14] modified a model for critical head to avoid

---

* Corresponding author.

failure due to piping. Estabragh et al. [15] investigated the effect of random reinforcement on the seepage velocity and seepage force in silty soil. Su et al. [16] introduced a particle flow code (PFC)-based approach to implement the numerical simulation for seepage behavior in soil levee and investigate the mesoscale seepage failures.

Throughout the domestic and international research of the piping effect, most of the scholars simulated and studied the formation mechanism and influencing factors of the piping phenomenon from the aspects of hydraulic gradient, seepage velocity, filter characteristics, grading curve, and the theory of particle flow [17–20]. These studies mainly focus on the macroscopical and semi-quantitative research on the formation and deterioration of piping. In the process and development of the piping effect, the mechanical mechanism of the interaction between soil particles and water flow are extremely complex, and because of high randomicity and influence factors, it is difficult to accurately calculate and fully express this process with a single equation or granular flow software. This paper combined the project of the Anqing–Hefei product oil pipeline crossing Hangbu River, considering the flood level and river erosion factors in a certain area, both the velocity field of groundwater seepage was simulated and the characteristics of which were analyzed by the Visual Modflow software. On the basis of the subbase, we evaluated the possibility of engineering inducing seepage damage.

2. Methods

2.1. Project profile

China Petrochemical Co., Ltd. intends to invest a new project of Anqing–Hefei petroleum products pipeline, which will be laid by Tongcheng–Feixi from south to north, among them, the pipeline project in Feixi county needs to cross Hangbu River. The overall perspective of crossing river and schematic of the pipeline entry point is shown in Fig. 1.

2.1.1. Basin profiles

As a tributary of Chaohu Lake, one of the five largest freshwater lakes in China, the Hangbu River is located in the central Anhui province, which has a complex topography, varied landform types, obvious features of mountain, hill, and plain. The area of the project is the humid subtropical monsoon climate, the average annual rainfall is 900–1,200 mm, and the average evaporation capacity over the years is 1,300–1,500 mm. According to the annual monitoring data from the Anhui hydrology bureau, the maximum and minimum flow rate of Hangbu River are 561 and –20.2 m^3/s, respectively; the maximum water level is 14.43 m and the lowest is 6.11 m. The geological situation of the pipeline crossing region is the loose Quaternary strata in the depth range of 0–19.4 m, which the top-down formation structure is plain fill, silt, medium sand, silty clay, medium sand stratum, silty clay, medium sand stratum, and silty clay in turn.

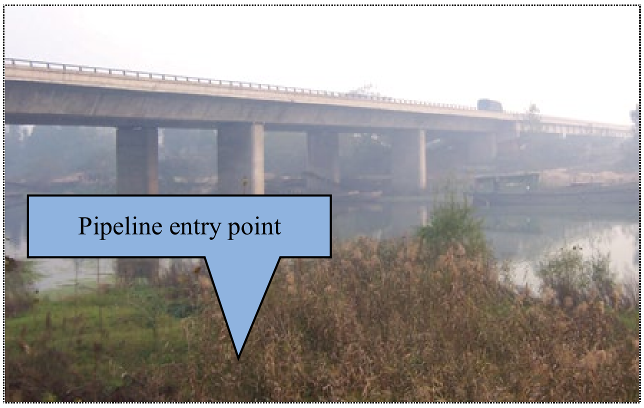

Fig. 1. The overall perspective of crossing river and schematic of pipeline entry point.

2.1.2. Pipeline crossing project

Anqing–Hefei oil pipeline project has been designed with a throughput of 750, 000 tons annually, and the final is 1.2 million tons. The pipe of the crossing Hangbu River is ϕ273.1 × 7.1 steel pipe which is 7.0 Mpa in designed pressure; Across the river, the width is about 240 m and the water surface is about 135 m, the water depth is about 5 m, and the length of the crossing is 491 m; In addition, the penetrating angle of south bank is 10° and the unearthed angle of the north bank is 6°, The channel of crossing region is basically straight, the elevation of the river bed and stream gradient are about 2 m and 0.2‰. Fig. 2 indicates the construction process with crossing pipeline. According to the Flood Control Standard (GB50201-2014) and the flood situation of a river basin, the preliminary design of the reinforcement works for the Hangbu River embankment is carried out by 20 year return period. The design standard of a project such as the embankment elevation is 17.5 m, the top width is 6.0 m, the bottom width is 90–130 m, the internal and external slope ratio is 2.0/2.0.

2.2. Hydrological computation

2.2.1. Storm flood

In Chaohu Lake, storm flood in various rivers are concentrated in May–October annually, the runoff is very great with long time and high water levels. There are three types of rainstorm flood type in Hangbu River: Backward flow, Top-lifted flow, and fluent flow. When the water level of the Yangtze River was higher than the inland river, which was poured into the center of the basin through Yuxi River, the flood in 1954 was this kind of Backward flow; When the water levels rose in the lower reaches of the Yangtze and Chaohu at the same time, the water logging would be occurred as for the influence of the top river, the flood appeared in 1949 and 1995 were the Top-lifted flow; When the water level of the rainstorm was low in the upper reach of Yangtze River, in the same period, there was heavy rain and the water level of the river had risen sharply, the flood in 1991 was the Fluent flow.

2.2.2. Stability of engineering reach

Due to the lack of section data of different periods in the river section where the project is located, only the measured

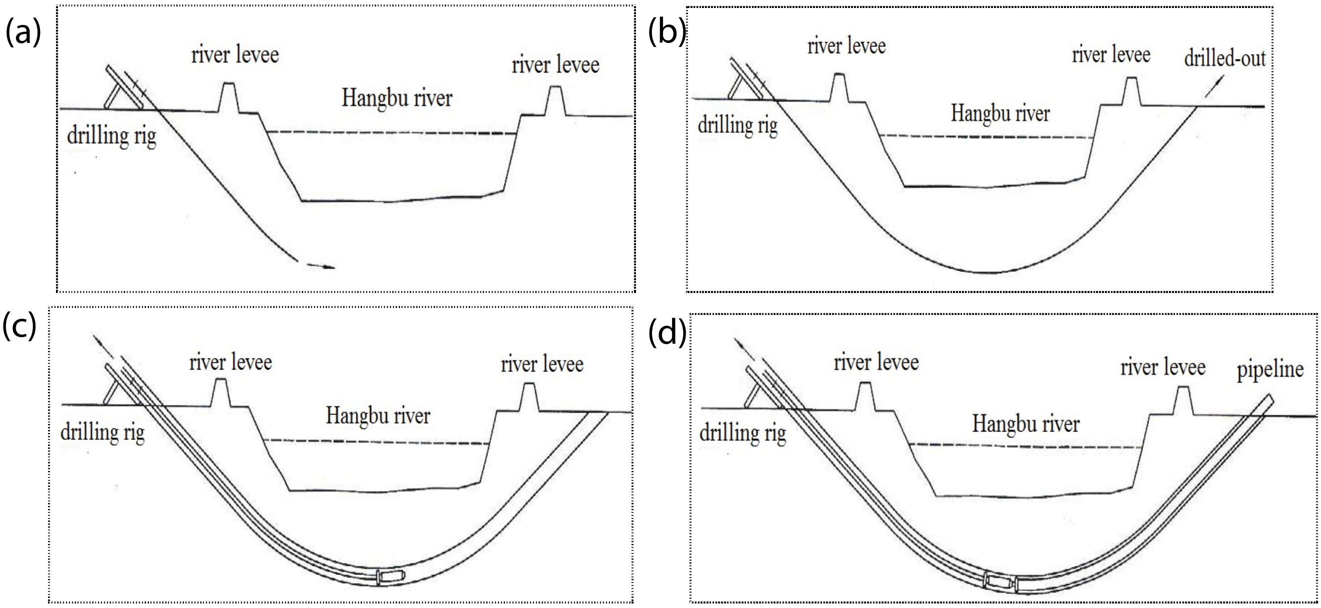

Fig. 2. The schematic of construction process with crossing pipeline. (a) Directional drilling, (b) drilled-out of pilot hole, (c) the pre-reaming, and (d) enlarge boring and pull-back of pipeline.

section of this evaluation is available. Therefore, it is difficult to make quantitative analysis and judgment on the longitudinal and horizontal deformation of the river, and only qualitative description can be made based on the width and depth relationship of the measured section. Eq. (1) is as follows,

$$\zeta = \sqrt{\frac{B}{H}} \quad (1)$$

where ζ is the transverse stability coefficient of the riverbed, B is the river width at the bed-making flow rate (m), H is the average water depth at the bed-making flow rate (m).

According to the above Table 1, the larger ζ value is, the wider and shallower the channel is, the more unstable the riverbed is, and vice versa [21]. Hangbu River project section is a plain river which is basically straight, where B is 135 m, H is 5 m, the stability coefficient ζ is calculated to be 2.32 less than 3, so the project river section belongs to the stable river section.

2.2.3. The design flow and the design water level

According to the Report of Flood Control Planning in Chaohu Basin (Anhui Survey and Design Institute of Water Conservancy and Hydropower, 2004), The designed flood about the different return periods of each point in Hangbu River are shown in Table 2.

The crossing pipeline project of Hangbu River is near to the Guanghan bridge. Based on the importance of pipeline engineering, the section of design flow and the water level could just adopt the data from the Chaohu Flood

Table 1
Stability parameters of various river sections

Type of river section	Stability coefficient		Stability	
	ϕ	ζ	Rank	Degree
Mountainous-valley river	14–90	2–4	1	
Mountainous-open river	4.9–55	3–5	2,3	Stability
Plain-straight river	0.37–2.2	3–4	2,3	
Plain braided stream	/	6	3,4	
Plain constraint bending	0.25–19.2	6–17	3	General stability
Plain free bending			4	
Wandering reach	0.17–1.3	20–40	5	
Mobile-bed river	1–24.4	5–12	5	Instability
Bahada river	/	15–32	6	
Delta river mouth			5	

Table 2
The designed flood in Hangbu River basin

Calculated points	Basin area (km^2)	Peak discharge (m^3/s)		Discharge modulus (m^3/s/km^2)	
		10 year return period	20 year return period	10 year return period	20 year return period
Jiangjun dam	1,810	1,650	1,850	0.916	1.022
Guanghan bridge	1,900	1,660	1,960	0.874	1.032
Datang bay	1,970	1,700	2,100	0.863	1.066
Lake entrance	4,150	2,480	2,980	0.598	0.719

Control Manual [22], so the values of which are 16.4 m and 1,960 m^3/s.

2.3. Numerical simulation of groundwater seepage field

2.3.1. Model overview

Combined the hydrological computation with the engineering geological conditions of the region, numerical simulation of the groundwater seepage field near the crossing river during the flood is simulated. Among them, the hydrological conditions are generalized as following [23–25]. Firstly, in the case of flood conditions with 20 year return period, the height of the embankment is not less than 16.4 m when the height of the embankment of the river is lower than the design flood level. Secondly, the stratigraphic strata near the channel are treated isotropic by non-homogeneous. Thirdly, according to the strata exposed by the existing borehole, the empirical value that the hydraulic conductivity of the intermediate fine sand in the strata is 1–20 m/d and the silty clay is less than 1 m/d. Lastly, when washed out of the riverbed, the vertical permeability coefficient is the same as the horizontal one.

2.3.2. Connectional hydrogeological model

In order to control the dynamic change of groundwater level and reflect the hydrogeological characteristics of research area, the scope of the region is mainly within 1,000 m of the construction site, which the span of east-west and north-south are both 2,000 m. The entire study area was divided into 40 × 40 grids, particularly, a grid subdivision was conducted where the river and the pipeline pass. The detailed grid division is shown in Fig. 3, in which the blue line is the channel and the black line is the pipeline. The stability of the river bed could be roughly predicted by the seepage velocity of groundwater in the pipeline wall during designed flood, the main parameters of the model are shown in Table 3. When calculating, the hydraulic conductivity is generally 10 m/d in the area and which is 1.5 times at crossing pipeline than other areas.

The pipe across the channel is bent at the bottom of the river, so as to make the model consistent with the actual situation, the strata are divided into five layers. The permeability coefficient of the place where the pipeline crossing is determined to be 1.5 times that of other areas. The specific stratigraphic distribution is shown in Fig. 4, in which the dyke is generalized into a vertical cubic shape. This model mainly predicts the impact of flood, as to simplify the model, the rainfall and evaporation amount offset each other as zero, the topography of the region is relatively flat, and the initial water head of the region is generalized to be horizontal.

2.3.3. Mathematical model and solution

According to the above hydrogeology conceptual model, the corresponding numerical model can be established as Eqs. (2)–(5).

$$\frac{\partial}{\partial x}\left(K_{xx}\frac{\partial H}{\partial x}\right)+\frac{\partial}{\partial y}\left(K_{yy}\frac{\partial H}{\partial y}\right)-W=\mu\frac{\partial H}{\partial t} \tag{2}$$

$$H(x,y,t)\big|_{t=0}=H_0(x,y)\quad (x,y)\in D \tag{3}$$

$$H(x,y,t)\big|_{\Gamma_1}=H_1(x,y,t)\quad (x,y)\in \Gamma_1 \tag{4}$$

$$\left.\frac{\partial H}{\partial n}\right|_{\Gamma_2}=0 \tag{5}$$

where K_{xx} and K_{yy} are the hydraulic conductivity in the direction of x and y, respectively (m/d), H is the groundwater level (m), W is the unit volume flow (m^3), μ is specific yield, H_0 is the initial water level of groundwater (m), H_1 is the groundwater level at the simulated boundary (m), t is time (d), D is the simulation area, Γ_1 is the first-class boundary of head loss, Γ_2 is the second type of flowrate boundary, and n is outside of the boundary normals.

The numerical simulation is solved by the finite difference method [26–30]. In calculating the water level of each unit in a finite-difference grid, a finite difference equation is established for each unit with the water balance between a node and its four adjacent nodes, then the water level is calculated by the conjugate gradient method. The general form of difference Eq. (6) is as follows:

$$b_{ij}H_{i-1,j}+d_{ij}H_{i,j-1}+e_{ij}H_{i,j}+f_{ij}H_{i,j+1}+g_{ij}H_{i+1,j}=q_{ij} \tag{6}$$

Show it by matrix notation of Eq. (7):

$$A\cdot x=b \tag{7}$$

where A is the coefficient matrix, x is water level matrix of each cell, b is flow rate which is connected with boundary of fixed water level and moisture storage capacity in a table cell.

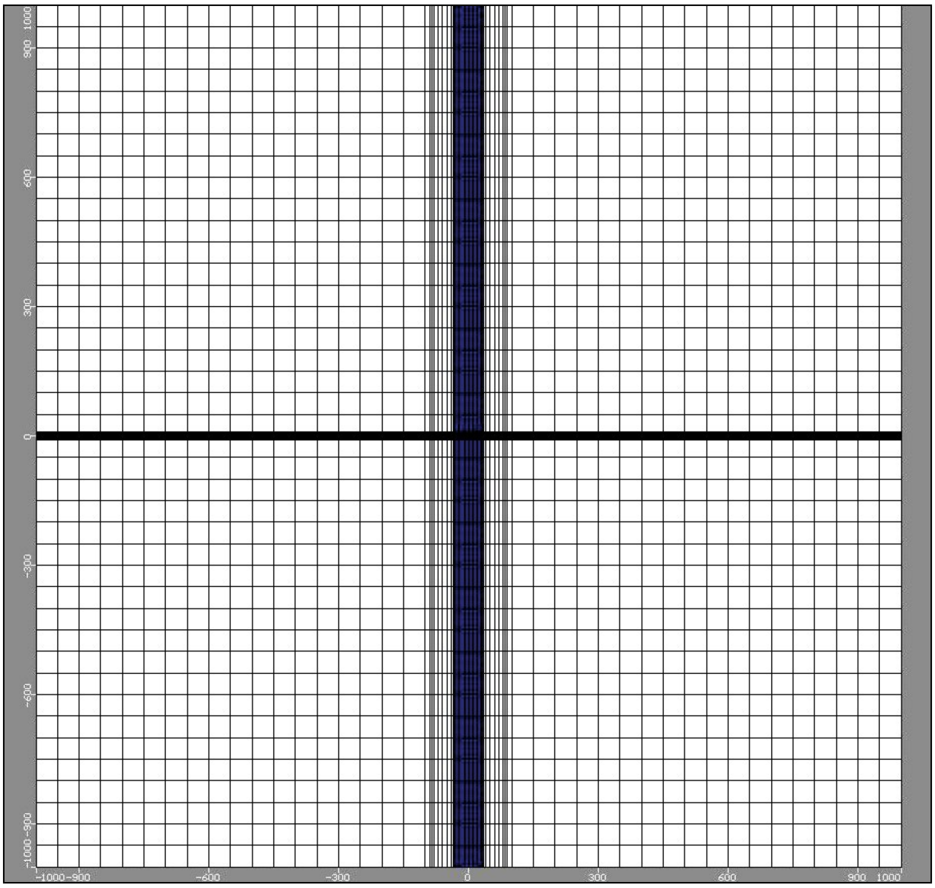

Fig. 3. Plane grid division of study area.

Table 3
Main parameters of model

Hydraulic conductivity (m/d)	10
Elastic storativity	0.0005
Specific yield	0.2
Porosity	0.4

3. Results and discussion

3.1. River-bed scour analysis

To check the depth of the pipeline below the river bed, it is necessary to analyze the maximum scour depth of the river in the design flood condition. According to the drilling data of pipeline engineering, bed soil is silty fine sand. The calculation formula of water scouring is used for the constant flow of non-viscous soil, as show in Eqs. (8) and (9). The calculation assumes that the banks on both sides of the river virtual heightening, in the design flood condition, the maximum scour depth calculation results of the channel in the engineering section are shown in Table 4.

$$q_{\max} = c_j \frac{Q_c}{B_c}\left(\frac{h_{\max}}{h_{\mathrm{pj}}}\right)^{5/3} \tag{8}$$

$$c_j = \left(\frac{B^{0.5}}{h}\right)^{0.15} \tag{9}$$

where c_j is concentration coefficient of unit discharge, Q_c is the flow rate of the main channel, which distributed by flow modulus (m^3/s), B_c is the width of main channel water (m), B is the river width of bed flow (m), h is the average depth of bed flow (m), $h_{\max}$ is the maximum depth of the main channel (m), h_{pj} is the average depth of the main channel (m), $q_{\max}$ is the maximum single-width flow (m^3/s/m).

When the riverbed material is non-cohesive soil, the formula for calculating the maximum depth after scouring is shown in Eq. (10).

$$h_s = \frac{q_{\max}}{v_c}\left(\frac{q_{\max}}{kd^y}\right)^{\frac{1}{1+x}} \tag{10}$$

where v_c is the critical velocity could be calculated by Sharmov formula (m/s), d is the average grain size of sediment in the channel (mm), k, y, and x are constant coefficients with values of 4.6, 1/3, and 1/6, respectively.

When the riverbed material is viscous soil, the formula for calculating the maximum depth after scouring is shown in Eq. (11).

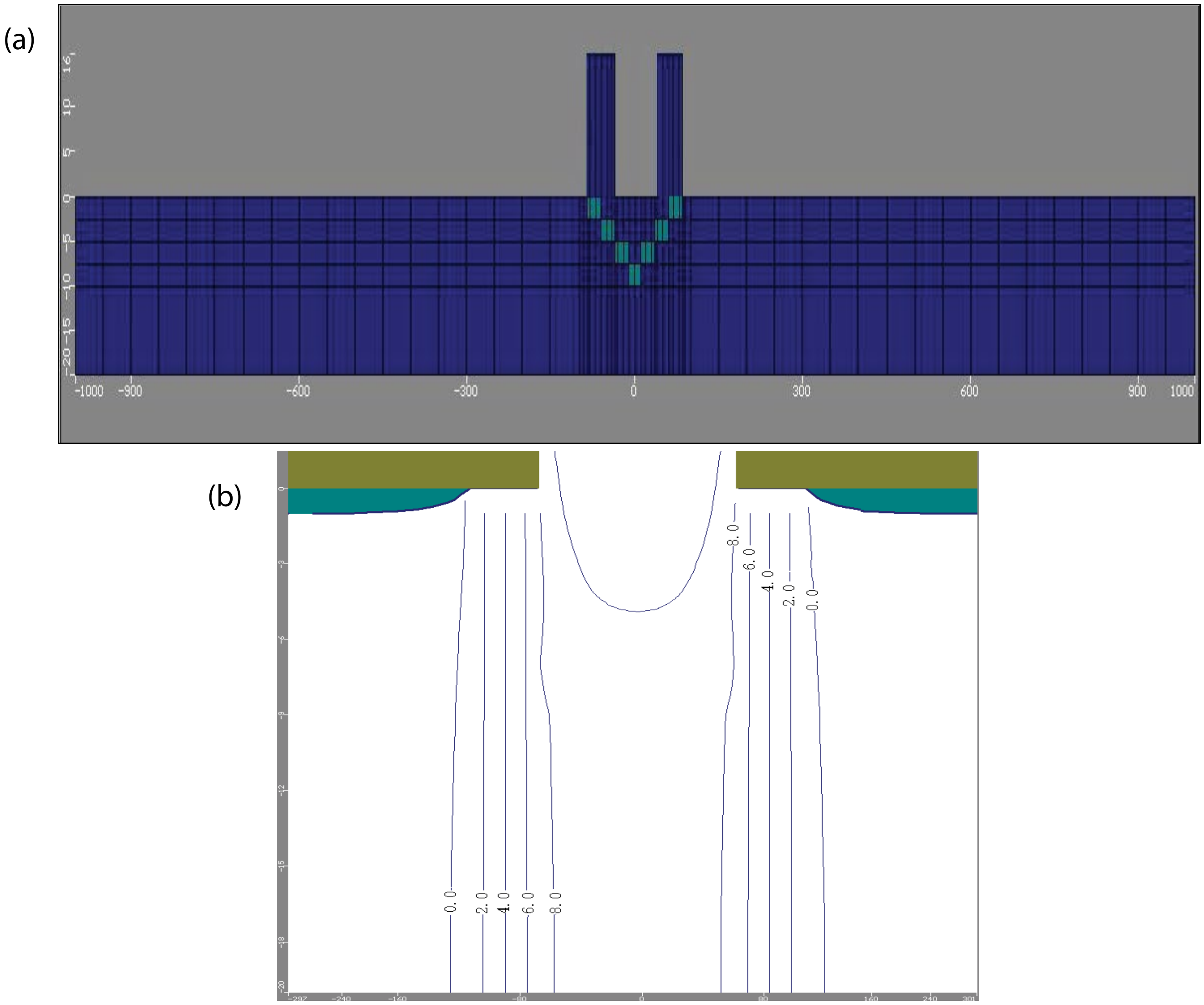

Fig. 4. (a) Vertical grid subdivision of study area and (b) section map of distribution of flow field.

Table 4
The calculated results of channel in designed flood conditions

Water level (m)	16.4
Sectional area (m^2)	1190
Flow rate (m^3/s)	1960
Average depth (m)	6.5
Maximum water depth (m)	9.13
Maximum scour depth (m)	2.28

$$h_s = \frac{q_{\max}}{v'_c} \tag{11}$$

where v'_c is the critical velocity could be calculated by Sharmov formula (m/s).

The calculation reflected that the river basin was scoured under the design flood condition. The maximum scour depth of the channel was 2.28 m, and the yellow sea elevation of the minimum scouring line was –0.78 m.

3.2. Numerical simulation results

After the model and parameter identification, groundwater simulation was conducted with the water level of 20 y return period, and the simulation period was 1 month. The model simulation results showed that the maximum hydraulic gradient of groundwater seepage in the flow field is $I_m = 0.148$. The distribution of groundwater flow field is shown in Figs. 4 and 5.

The maximum hydraulic gradient of model was obtained through the operation and calculation, in which the available hydraulic gradient could be calculated by the following Eqs. (12) and (13).

$$I_{ac} = \frac{I_{cr}}{K} \tag{12}$$

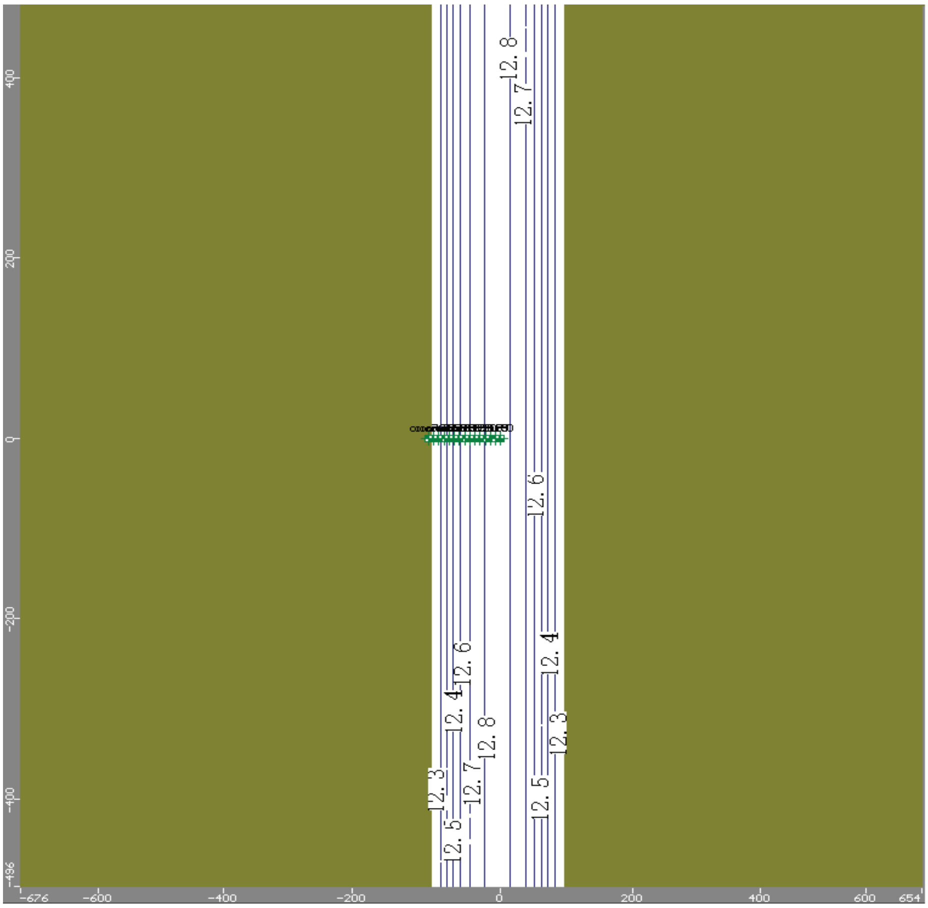

Fig. 5. The plane graph of distribution of flow field.

$$I_{\mathrm{cr}} = \frac{r}{r_w} = \left(G_s - 1\right)\left(1 - n\right) \tag{13}$$

where I_{ac} is the available hydraulic gradient, I_{cr} is the critical hydraulic gradient, K is the safety factor, which the average value is 2.0–2.5, n is soil porosity.

According to the numerical simulation results, the maximum hydraulic gradient of groundwater seepage in flow field is $I_m = 0.148$, the available hydraulic gradient is calculated as $I_{\mathrm{ac}} = 0.369$; on account of $I_m < I_{\mathrm{ac}}$, that is to say the maximum hydraulic gradient in the underground flow field is less than the minimum hydraulic gradient required for the disturbed sand grains.

3.3. Results analysis

According to the maximum seepage velocity in the groundwater flow field and the engineering geological conditions of the project stratum, the perturbation ability of the seepage velocity to the loose particles in the stratum is judged. As to the above simulation results and the groundwater flow field profile in Fig. 4 and the groundwater flow field plane in Fig. 5, the pipeline crossing the embankment changes the regional groundwater flow field. Considering that the pipeline project increases the seepage velocity of surrounding strata by 50%, the seepage velocity in the groundwater flow field is less than the minimum seepage velocity required by the disturbed sand grains. That is, the maximum hydraulic gradient in the groundwater flow field is less than the allowable hydraulic gradient [31–35]. Therefore, considering riverbed erosion and the possibility of piping induced by groundwater seepage under the condition of high water level is relatively small, pipeline crossing will not have a destructive influence on the anti-slip and seepage stability of embankment design.

In addition, channel erosion has a certain impact on pipeline burial depth. Under the condition of design standard flood, the maximum flushing depth of the channel in Hangbu River is 2.28 m, and the Yellow Sea elevation of the lowest scouring line is –0.78 m. The design of pipeline bottom under the riverbed is 6 m below the riverbed, and the design elevation of pipeline bottom is –7.5 m, the pipeline is below the minimum scour line, which can meet the requirements of "code for design of oil and gas transportation pipeline crossing engineering" (GB50423-2013) that the covering layer is greater than 1.5 m. The buried depth of the pipeline complies with the provisions of article 5.5.2 of "Standard for flood control" (GB 50201-2014), that is, the buried depth of water, oil, gas, and other pipeline projects crossing through the bottom of the water (rivers and lakes) should be below the scour depth of corresponding flood control standard.

Although the buried depth of the pipeline meets the requirements, the crossing project has a certain impact on the seepage stability of the embankment, after the construction of a pipeline, seepage prevention should be carried out at the soil entry point and the unearthed point.

4. Conclusions

- The stability of river embankments will be affected by pipeline crossing engineering, therefore, the seepage stability analysis is required. In the study of this project, the Hangbu River crossing pipeline is arranged outside the design section of the embankment, the maximum hydraulic gradient of groundwater seepage is $I_m = 0.148$, and the maximum scour depth is 2.28 m with the yellow sea elevation of the minimum scouring line is –0.78 m, so the maximum hydraulic gradient calculated by numerical model is less than the available hydraulic gradient. In the process of engineering implementation, there are no cases of damage to existing embankments and regional stratigraphic permeability, the pipeline crossing is not destructive to the design of river embankments. Besides, the riverbed in flood season can be washed without causing the seepage damage of the project area.
- The change of hydraulic gradient will affect the extent of the seepage damage to the embankment in the early and later stages of the project, how to combine the theory of fine particle flow and visualization technique to study the interaction mechanism of soil and water near the pipeline, and accurate prediction of piping and seepage failure cycle, This is a research work that needs to be focused on later.
- Based on the establishment of the hydrogeological model, the Modflow software can be used to simulate the pipeline crossing engineering and provide a reference for the prediction and evaluation of the similar embankment project. However, due to the lack of model simulation, it is difficult to comprehensively consider the rules of the formation and development of piping from the perspective of the fluid-structure interaction mechanism of soil in the mesoscopic level [36–40]. Moreover, the hydraulic mechanism of local piping and the tubular seepage in the soil is still to be further studied and discussed in the future.

Acknowledgments

This research work was financially supported by the key project of Natural Science Foundation of Anhui (No. KJ2017A409), the key Provincial Teaching Research Project of Anhui (No. 2017jyxm0384), and supported by Natural Science Foundation of West Anhui University (No. WXZR201618).

References

[1] L.Q. Ding, D.Y. Sun, Study on some key tasks in dike engineering, Water Resour. Dev. Res., 2 (2002) 59–62.

[2] Y.L. Luo, B.Y. Su, J.C. Sheng, M.L. Zhan, New understandings on piping mechanism, Chin. J. Geotech. Eng., 33 (2011) 1895–1902.

[3] S. Wang, J.S. Chen, D.W. Huang, W.Z. He, H.Q. He, Experimental study on piping development considering effect of foundation structure, Chin. J. Geotech. Eng., 35 (2013) 2334–2341.

[4] J.S. Chen, H. Zhang, S. Wang, W.Z. He, K.L. Yuan, Experimental researches on effect of foundation structure on piping in multi-layer embankment, Chin. J. Geotech. Eng., 36 (2014) 2213–2219.

[5] J. Liu, D.S. Xie, Y.H. Cui, Failure mechanism of seepage in levees with double-layer foundation, J. Hydraul. Eng., 39 (2008) 1211–1220.

[6] Y. Liang, J.S. Chen, L. Chen, J.Q. Shen, Laboratory tests and analysis on piping in two-stratum dike foundation, Chin. J. Geotech. Eng., 33 (2011) 624–629.

[7] G.X. Li, X.J. Zhou, Laboratory simulation on generation and evolution of piping in embankment foundation, Adv. Sci. Technol. Water Resour., 25 (2005) 21–24.

[8] J. Zhou, Z.X. Yao, G. Zhang, Meso-laboratory study on initiation and evolution of piping, Chin. J. Underground Space Eng., 3 (2007) 842–848.

[9] Y. Wang, Q. Dong, Y. Chen, Seepage simulation using pipe network flow model in a discrete element system, Comput. Geotech., 92 (2017) 201–209.

[10] J. Ubilla, T. Abdoun, L. Sasaakul, M. Sharp, S. Steadman, W. Vanadat-Ellis, New Orleans Levee system performance during hurricane Katrina, London Avenue and Orleans Canal South, J. Geotechn. Geo Environ. Eng., 134 (2008) 668–680.

[11] K. Fujisawa, A. Murakami, S. Nishimura, Numerical analysis of the erosion and the transport of fine particles within soils leading to the piping phenomenon, Soils Found., 50 (2010) 471–482.

[12] X.J. Zhou, Y.X. Jie, G.X. Li, Numerical simulation of the developing course of piping, Comput. Geotech., 44 (2012) 104–108.

[13] D.Y. Wang, X.D. Fun, Y.X. Jie, W.J. Dong, D. Hu. Simulation of pipe progression in a levee foundation with coupled seepage and pipe flow domains, Soils Found., 54 (2014) 974–984.

[14] C.S.P. Ojha, V.P. Singh, D.D. Adrian, Determination of critical head in soil piping, J. Hydraul. Eng., 129 (2003) 511–518.

[15] A.R. Estabragh, A. Soltani, A.A. Javadi, Models for predicting the seepage velocity and seepage force in a fiber reinforced silty soil, Comput. Geotech., 75 (2016) 174–181.

[16] H.Z. Su, Z.Q. Fu, A. Gao, Z.P. Wen, Particle flow code method-based meso-scale identification for seepage failure of soil levee, Transp. Porous Media, 119 (2017) 311–336.

[17] D.J. Hagerty, A. Curini, Impoundment failure seepage analyses, Environ. Eng. Geosci., 1 (2004) 57–68.

[18] X.D. Ni, Y. Wang, F. Wang, Study on piping by sand-bank model and simulation by PFC3D, J. Sichuan Univ., 41 (2009) 51–57.

[19] G.L. Sivakumar Babu, A.K. Vasudevan, Seepage velocity and piping resistance of coir fiber mixed soils, J. Irrig. Drain. Eng., 134 (2008) 485–492.

[20] O. Kohei, T. Kenji, S. Yutaka, I.L. Hoe, K. Toshinori, Fluid coupled-DEM simulation of lateral loading experiment for buried pipe in saturated sand, Transp. Infrastruct. Geotechnol., 5 (2018) 93–113.

[21] Third Survey and Design Institute, MOR, Hydrology and Bridge Crossing, China Railway Press, Beijing, 1999.

[22] Chaohu Water Conservancy Bureau, Chaohu Flood Control Manual, Anhui Provincial Flood Control and Drought Relief Headquarters, Hefei, 2010, p. 63.

[23] P. Vazouras, S.A. Karamanos, Structural behavior of buried pipe bends and their effect on pipeline response in fault crossing areas, Bull. Earthquake Eng., 15 (2017) 4999–5024.

[24] A. Gupta Das, M.S. Babel, S. Ashrafi, Effect of soil texture on the emission characteristics of porous clay pipe for subsurface irrigation, Irrig. Sci., 27 (2009) 201–208.

[25] S.S. Abedi, Failure investigation of a defective weldment of an oil product transmission pipeline, J. Fail. Anal. Prev., 17 (2017) 30–37.

[26] S.Y. Feng, G.Y. Gao, Z.L. Huo, H.B. Zhan, Semi-analytical solution for reactive solute transport in the convergent flow to an extraction well considering scale-dependent dispersion, J. Hydraul. Eng., 41 (2010) 1024–1031.

[27] A. Jafar Ahamed, K. Loganathan, Water quality concern in the Amaravathi River Basin of Karur district: a view at heavy metal concentration and their interrelationships using geostatistical and multivariate analysis, Geol. Ecol. Landscapes, 1 (2017) 19–36, doi: 10.1080/24749508.2017.1301055.

[28] G. Theotokatos, K. Sfakianakis, D. Vassalos, Investigation of ship cooling system operation for improving energy efficiency, J. Mar. Sci. Technol., 22 (2017) 38–50.

[29] Y. Han, J. Li, X. Yang, W. Liu, Y. Zhang, Dynamic prediction research of silicon content in hot metal driven by big data in blast furnace smelting process under hadoop cloud platform, Complexity, 2018 (2018) 1–16.

[30] T.S. Muhammad, Z. Hanhui, A. Muhammad, Y. Jia Xin, R. Li, Effects of different type of black smoke originate from kilns on the natural environment, J. Clean WAS, 3 (2019) 11–13.

[31] K.S. Richards, K.R. Reddy, Critical appraisal of piping phenomena in earth dams, Bull. Eng. Geol. Environ., 66 (2007) 381–402.

[32] M. Foster, R. Fell, M. Spannagle, A method for assessing the relative likelihood of failure of embankment dams by piping: reply, Can. Geotech. J., 39 (2002) 497–500.

[33] S.S. Lam, R.K. Liew, Y.M. Wong, E. Azwar, A. Jusoh, R. Wahi, Activated carbon for catalyst support from microwave pyrolysis of orange peel, Waste Biomass Valorization, 8 (2017) 2109–2119.

[34] S.S. Lam, N.L. Ma, A. Jusoh, M.A. Ambak, A study on the optimal tank design and feed type to the growth of marble goby (*Oxyeleotris marmorata* Bleeker) and reduction of waste in a recirculating aquaponic system, Desal. Water Treat., 52 (2014) 1044–1053.

[35] S.S. Lam, M.A. Ambak, A. Jusoh, A.T. Law, Waste excretion of marble goby (*Oxyeleotris marmorata* Bleeker) fed with different diets, Aquaculture, 274 (2008) 49–56.

[36] J.E. Cheng, Implication of reservoir characteristics based on overview of structure and sedimentology of outcrops along Bintulu-Niah-Miri areas, Malaysian J. Geosci., 3 (2019) 12–22.

[37] X.J. Zhou, Y.X. Jie, G.X. Li, Numerical simulation of piping based on coupling seepage and pipe flow, Rock Soil Mech., 30 (2009) 3154–3158.

[38] A.Md. Nazmul, C. Bo-Ching, Sustainable water treatment management, Water Conserv. Manage., 3 (2019) 11–13.

[39] C.X. Mao, X.B. Duan, J.B. Cai, J.H. Ru, Theoretical analysis of piping development of levee foundation, J. Hydraul. Eng., 35 (2004) 46–50.

[40] N.F. Zephania, J.P.T. Suiven, F. Martin, Eucalyptus tree colonization of the Bafut-Ngemba forest reserve, north west region, Cameroon, Environ. Ecosyst. Sci., 3 (2019) 12–16.